

# Bimodal decompression sickness onset times are not related to dive type or event severity

Amy E. King<sup>1</sup>, F. Gregory Murphy<sup>1,2</sup>, Laurens E. Howle<sup>1,3,4,†</sup>

<sup>1</sup>Department of Mechanical Engineering and Materials Science  
Hudson Hall, Research Drive  
Duke University  
Durham, NC 27708-0300 USA

<sup>2</sup>Navy Experimental Diving Unit  
321 Bullfinch Road  
Panama City, FL 32407-7015 USA

<sup>3</sup>Department of Radiology  
Box 3808 DUMC  
Duke University Medical Center  
Durham, NC 27710-4000 USA

<sup>4</sup>BelleQuant Engineering, PLLC  
7813 Dairy Ridge Road  
Mebane, NC 27302-9281 USA

†Corresponding author: [laurens.howle@duke.edu](mailto:laurens.howle@duke.edu), 919.660.5336

Keywords: Decompression sickness, Decompression illness, Unimodal, Bimodal, Occurrence density  
function, Symptom onset time, Survival analysis

## 29 Abstract

30 Human decompression sickness (DCS) is a condition associated with depressurization during underwater  
31 diving. Human research dive trial data containing dive outcome (DCS, no-DCS) and symptom information  
32 are used to calibrate probabilistic DCS models. DCS symptom onset time information is visualized using  
33 occurrence density functions (ODF) which plot the DCS onset rate per unit time. For the BIG292 human  
34 dive trial data set, a primary U.S. Navy model calibration set, the ODFs are bimodal, however probabilistic  
35 models do not produce bimodal ODFs. We investigate the source of bimodality by partitioning the BIG292  
36 data based on dive type, DCS event severity, DCS symptom type, institution, and chronology of dive trial.  
37 All but one variant of data partitioning resulted in a bimodal or ambiguously shaped ODF, indicating that  
38 ODF bimodality is not related to the dive type or the DCS event severity. Rather, we find that the dive  
39 trial medical surveillance protocol used to determine DCS symptom onset time may have biased the  
40 reported event window. Thus, attempts to develop probabilistic DCS models that reproduce BIG292  
41 bimodality are unlikely to result in an improvement in model performance for data outside of the  
42 calibration set.

43

## 44 Introduction

45 Decompression sickness (DCS) is a condition associated with depressurization of the body from  
46 underwater diving. During a dive, exposure to increased ambient pressure allows elevated partial  
47 pressures of inert gas in the lung to dissolve into the blood. When this blood circulates, the inert gas can  
48 diffuse into the body's tissues. During decompression and after surfacing from a dive, the excess inert gas  
49 is normally circulated back to the lungs to be exhaled. However, if the ambient pressure is reduced  
50 sufficiently far below the partial pressure of the dissolved gases, then gaseous bubbles may form in the  
51 blood and/or tissues. The signs and symptoms of DCS can include, but are not limited to joint pain,  
52 paresthesia, fatigue, abdominal pain, and paralysis [1]. DCS cases are typically categorized into either  
53 Type I (also called mild) or Type II (also called serious), in which Type I includes pain-only cases and Type  
54 II includes neurological and cardiopulmonary cases. In addition, DCS manifestations which subsequently  
55 spontaneously resolve without recompression treatment are categorized as marginal DCS cases.  
56 Examples of marginal cases are pain in one joint lasting less than 60 minutes or pain in two joints lasting  
57 less than 30 minutes [2, 3].

58 Decompression modeling originated in the early 20<sup>th</sup> century when Boycott *et al.* introduced the  
59 theory that DCS was caused by the formation of bubbles in the body during decompression due to the  
60 elevated partial pressure of dissolved nitrogen gas in the body's tissues [4]. The model presented by  
61 Boycott and coworkers, later known as the Haldane model, was deterministic, as DCS could be avoided if  
62 a set of criteria were followed and was inevitable if those criteria were violated. However, deterministic  
63 modeling cannot account for the variation in DCS occurrence and symptoms present in divers executing  
64 identical dive profiles as recorded in empirical dive data [2, 3]. This variability in DCS outcome prompted  
65 the development of probabilistic models, introduced by Berghage *et al.* [5] and Weathersby *et al.* [6],  
66 which compute a non-zero probability of DCS occurrence for a given dive profile. Such probabilistic

67 models used to predict the incidence and onset time of DCS rely on risk calculated from survival analysis  
68 [7] and either a gas content or bubble model . These models allow dive profiles to be created with a level  
69 of risk tailored to the diver's objective. An advantage of probabilistic modeling is that their parameters  
70 can be calibrated with empirical dive data via numerical optimization. Model parameters can be  
71 estimated to maximize the likelihood, which is a statistic that quantifies the agreement between the  
72 model and the corresponding experimental data. In addition, including the time of onset of DCS  
73 symptoms from experimental data during optimization has been shown to improve a model's ability to  
74 describe the data [8]. To facilitate calibration of probabilistic DCS models with experimental dive data,  
75 Temple *et al.* published a compilation of dive profile and DCS manifestation descriptions corresponding  
76 to both air and nitrogen-oxygen human dive trials conducted by the United States, United Kingdom, and  
77 Canadian militaries between 1944 and 1997 [2, 3]. These research trials were conducted in hyperbaric  
78 chambers and include both wet and dry dives during which a medical officer monitored divers and  
79 determined the time of onset of DCS symptoms. Temple's report includes the bottom times, depths, and  
80 ascent rates which characterize each dive profile, and the corresponding dive conditions (wet or dry),  
81 inspired gas mixtures, DCS symptom descriptions and onset times, and references to the originating dive  
82 trial reports. The dive types performed during these research trials include single air, single non-air,  
83 repetitive and multilevel air, repetitive and multilevel non-air, air and oxygen decompression, saturation,  
84 sub-saturation, surface decompression with air, and surface decompression with oxygen . The calibration  
85 set known as the BIG292 standard DCS data set is a subset of the data presented by Temple *et al.* that  
86 includes a portion of the single air, single non-air, repetitive and multilevel air, repetitive and multilevel  
87 non-air, and saturation dive types. This calibration set has been used in optimizing the parameters for a  
88 probabilistic model known as the LE1-USN93 model [9]. The LE1 model consists of three perfusion-limited  
89 parallel compartments, two with mono-exponential gas uptake and elimination and one with mono-

90 exponential uptake and linear elimination after a crossover tension is exceeded [10]. The BIG292  
91 calibration data set is analyzed in the present work.

92 An occurrence density function (ODF) describes the number of occurrences of a particular event  
93 per unit of time, and can be used to graphically assess the agreement between a model's estimations and  
94 observed DCS occurrences and onset times. These plots map time relative to the final surface interval on  
95 the abscissa and the number of DCS occurrences on the ordinate. A probabilistic model that most  
96 accurately predicts the onset time of DCS would generate an ODF which closely resembles that of  
97 empirical dive data. The ODF constructed with the BIG292 dive data set is bimodal, peaking in DCS  
98 occurrences at both the completion of decompression and two hours following decompression. However,  
99 current probabilistic models, including the LE1-USN93 [9] and the BVM(3) [11], used to predict the onset  
100 time of DCS do not produce bimodal ODFs. The ODFs of the LE1-USN93 and BVM(3) models each contain  
101 only one peak, located after the completion of decompression. Simulating the bimodality of the empirical  
102 data would improve the fit of the model to the data, creating a better likelihood match.

103 Recently, Hada [12] investigated using inert gas input delay in a class of probabilistic  
104 pharmacokinetic models with perfusion coupled compartments [13] and perfusion-diffusion coupled  
105 compartments in an effort to align model onset time predictions with the bimodal onset times found in  
106 the BIG292 data. Of the 11 delay-differential probabilistic pharmacokinetic models Hada optimized and  
107 analyzed, many showed an improvement in model fit with the addition of the single-parameter input  
108 delay but none showed enough improvement by the Akaike Information Criterion to justify adding input  
109 delay. Additionally, none of the models, when optimized on the BIG292 data, predicted bimodal ODFs.  
110 This finding motivated our present study to investigate bimodality of the BIG292 dive data. We wish to  
111 know if there is a feature, such as dive type, event severity, symptom type, or breathing gas, generates  
112 the two peaks in the ODF. If so, this might inform what model changes could lead to improved onset time

113 prediction. If no feature can be identified, or if the bimodality is a result of some type of measurement  
114 bias, then attempts to reproduce bimodality in model prediction are unlikely to be successful or useful.

## 115 Methods

### 116 Data

117 The BIG292 standard DCS data set from two Naval Medical Research Institute (NMRI) reports was  
118 used [2, 3] in this study. The BIG292 data set, which is a subset of the dive data detailed in [2, 3], contains  
119 dive profiles from 3,322 exposures of air and nitrogen-oxygen diving conducted by the United States,  
120 United Kingdom, and Canadian militaries between 1944 and 1997. The BIG292 data set includes single  
121 air, single non-air, repetitive and multilevel air, repetitive and multilevel non-air, and saturation dive  
122 types, resulting in 190 DCS cases and 110 marginal DCS cases. Marginal DCS is defined as a case involving  
123 signs or symptoms associated with DCS that were deemed not serious enough to be treated with  
124 recompression and subsequently spontaneously resolved [2, 3]. In the BIG292 data set, all DCS cases and  
125 68 of the 110 marginal DCS cases are reported with symptom onset times  $T_1$  and  $T_2$ , where  $T_1$  is the last  
126 known time a diver was symptom free, and  $T_2$  is the earliest time the diver was definitely experiencing  
127 symptoms. Following our previous work on the efficacy of using marginal DCS events in fitting  
128 probabilistic DCS models, we scored marginal cases as non-events when considering the BIG292 data set  
129 in this work so that only full DCS events were analyzed [14, 15]. Because these dive trial data are de-  
130 identified and are freely available to the public in the form of two U.S. Government reports, IRB approval  
131 was not required for this retrospective study.

132 The 190 DCS cases in the BIG292 data set can be further classified by perceived severity index  
133 (PSI) [16, 17]. As introduced by Howle *et al.*, the PSI scale is defined with the following six indices, in order  
134 of increasing severity: constitutional (fatigue, nausea, dizziness), skin bends (rash, itching, marbling), pain  
135 (aches, joint pain, stiffness), mild neurological (numbness, paresthesia), cardiopulmonary (dyspnea,

136 cough, hemoptysis), and serious neurological (dysfunction of vision, hearing, bladder, bowel,  
137 coordination) [17]. Based on the DCS symptom descriptions in the two NMRI reports [2, 3], the 190 DCS  
138 cases were each assigned an index by Howle *et al.*, with 6 indicating constitutional and 1 indicating serious  
139 neurological. If a DCS case fell into more than one of these categories, it was assigned an index  
140 corresponding to the highest severity present. Traditionally, DCS is categorized into Type I (mild) and Type  
141 II (serious), where Type I includes the PSI categories of constitutional, skin, and pain, and Type II includes  
142 mild neurological, cardiopulmonary, and serious neurological manifestations. An alternative approach to  
143 classifying DCS severity was proposed by Howle *et al.* [17], called Type A/B splitting. Type A (mild) includes  
144 the PSI categories of constitutional, skin, pain, and mild neurological, while Type B (serious) includes the  
145 cardiopulmonary and serious neurological PSI categories. In the BIG292 data set, there are 152 cases of  
146 Type I DCS and 38 cases of Type II DCS. Applying Type A/B splitting, the BIG292 data set contains 170 Type  
147 A and 20 Type B DCS cases. When exploring DCS symptom type as a potential source of the bimodal ODF  
148 in this work, both Type I/II and Type A/B splitting were applied to the BIG292 data. DCS cases  
149 corresponding to each individual PSI were also examined.

## 150 Computational Modeling

151 Many probabilistic DCS models are derived using the methods of survival analysis [7]. For these  
152 models, the probability of DCS is defined as

$$153 \quad P(E) = 1 - e^{-\sum_i g_i \int r_i dt} \quad (1)$$

154 where  $P(E)$  is the probability of a DCS event occurring, the index  $i$  counts over the risk-bearing model  
155 compartments,  $g_i$  is the  $i^{th}$  compartmental gain,  $r_i$  is the  $i^{th}$  compartmental hazard function, and the  
156 definite integral containing the hazard function is evaluated from the beginning of the exposure to the

157 right censoring time. It should be noted that the risk function of the form of Eq. (1) assumes a time-  
 158 uniform event probability. Models differ by their definitions of compartmental hazard functions,  $r_i$ .

159 The event probability of DCS defined in Eq. (1) can be modified to include the time of symptom  
 160 onset (event window), which was first introduced into the field of probabilistic DCS modeling by  
 161 Weathersby *et al.* [8]. The BIG292 data define the DCS event window using times  $T_1$ , the last time the  
 162 diver was known to be symptom-free and  $T_2$ , the first time the diver was known to be symptomatic. For  
 163 a profile which results in DCS, the event probability can be expressed as

$$164 \quad P(E) = P(0)_{0 \rightarrow T_1} P(E)_{T_1 \rightarrow T_2} = e^{-\sum_i g_i \int_0^{T_1} r_i dt} \left( 1 - e^{-\sum_i g_i \int_{T_1}^{T_2} r_i dt} \right) \quad (2)$$

165 where  $P(0)_{0 \rightarrow T_1}$  is the probability that the diver remained asymptomatic from the beginning of the  
 166 exposure until time  $T_1$ , and  $P(E)_{T_1 \rightarrow T_2}$  is the probability that the diver is bent during the event window  
 167  $T_1 \rightarrow T_2$ . The event windowing information is also used in constructing the ODF, as explained below.

168 Although recent work has considered the use of Bayesian inference in optimizing probabilistic DCS  
 169 models [18], most models are optimized by maximizing the log likelihood function

$$170 \quad LL = \sum_{n=1}^N \ln \left( P(E_n)^{\delta_n} (1 - P(E_n))^{(1-\delta_n)} \right) \quad (3)$$

171 in order to find the best set of model parameters [6]. In Eq. (3),  $n$  counts over the  $N$  exposures and  
 172  $\delta_n = 1$  if the  $n^{th}$  exposure resulted in DCS and  $\delta_n = 0$  otherwise. Typically, marginal DCS cases are  
 173 assigned a fractional weight,  $\delta_n = 0.1$ , but as discussed above, we de-rate marginal DCS events to non-  
 174 events [14, 15].



175 Occurrence density functions that display both the experimentally observed and model estimated  
176 DCS onset can be used to visualize a model's agreement with dive trial data. The ODF of observed DCS  
177 data is calculated using convolution with a top hat function [19]. Time is divided into one-hour bins, where  
178 a top hat function is turned on at the start of each bin and off at the end of each bin. To generate the  
179 model-predicted ODF, the probability of a DCS occurrence in each individual bin is calculated with Eq. (2)  
180 (with  $T_1$  and  $T_2$  equal to the bin's time interval bounds) for a particular exposure. The sum of the  
181 probabilities for all exposures in each bin is plotted against time relative to the final surface interval to  
182 create the occurrence density function [10, 11].

### 183 Data Partitioning

184 In order to determine the cause of the bimodal peaks in the BIG292 dive data ODF, many different  
185 schemes for partitioning the data were examined. DCS occurrence density functions were computed and  
186 plotted with the data partitioned by dive type, DCS event severity, DCS symptom type, institution  
187 conducting the dive trial, and chronology of the dive trial data. Marginal DCS cases were not included in  
188 these ODFs, as they were scored as non-events; apart from one ODF which considers only marginal events.  
189 Each ODF was determined to be bimodal, unimodal, or ambiguous in shape by visual inspection of the  
190 number of peaks present. The BIG292 onset time bimodality could be attributed to dive type, event  
191 severity, symptom type, institution, or chronology if one of these methods of data partitioning resulted in  
192 unimodal ODFs. For reference, the onset time determination method was extracted from each dive report  
193 (Table 1) to determine post-dive medical protocol.

194 First, the BIG292 dive data files were categorized by dive type and breathing gas, which included  
195 single air, repetitive and multi-level air, single non-air, repetitive and multi-level non-air, and saturation  
196 (Table 2) [20]. The ODFs for a subset of the BIG292 data were examined using these dive type categories  
197 previously by Thalmann *et al.* [10], however they were not seeking to determine the cause of the bimodal

198 ODF. Dive profiles were also partitioned by event severity. Both Type I/II and Type A/B splitting were  
199 used, in which Type I and Type A are considered mild DCS, while Type II and Type B are considered serious  
200 DCS. The distribution of PSI classifications into each severity splitting method is summarized in Table 3.  
201 Next, DCS data were separated according to their PSI, and the number of DCS occurrences with each PSI  
202 are listed in Table 4.

203 The BIG292 dive data were then partitioned by originating dive report, followed with grouping by  
204 the institution that conducted each dive trial [2, 3]. The institutions included in the BIG292 data set are  
205 the Navy Experimental Diving Unit (NEDU), Naval Medical Research Institute (NMRI), Naval Submarine  
206 Medical Research Laboratory (NSMRL), Defense and Civil Institute of Environmental Medicine (DCIEM),  
207 and Institute of Naval Medicine (INM) (Table 5). Finally, the data were split by the year the dive trials  
208 were conducted and organized chronologically by end date (Table 6). Some dive trials spanned many  
209 years, so the corresponding data files were divided based on the date the data were collected. This  
210 chronological list was grouped into year ranges each containing similar quantities of DCS occurrences.  
211 These year ranges, which can be found in Table 6, are 1978-1983, 1984, 1985-1987, and 1988-1992, which  
212 include 44, 57, 43, and 46 DCS events respectively. There were two exceptions to this chronological  
213 method of data partitioning. First, though the dive trials contained in the DC4W data file spanned 1979-  
214 1986, all eight DCS events occurred during 1978-1983, so this data file was included in that chronology  
215 range. Second, the ASATNMR data file was composed of dive trials during June-August 1986, and then  
216 another during July 1988. The single DCS occurrence corresponding to these 50 dives occurred during the  
217 July 1988 dive trial, so the data from this file was included in the 1988-1992 range. ODFs were generated  
218 for each dive report, for all dive data generated by each institution, and for each of the year ranges  
219 outlined above.

## 220 Results

221 The DCS onset time measurement methods used in each dive report contributing to the BIG292  
222 data set are documented in Table 1. The NSMRL 1200 [21], NEDU 1-99/NMRC 99-01 [22], NMRI 86-97  
223 [23] technical reports all followed the same onset time determination procedure: divers were examined  
224 by a U.S. Navy Diving Medical Officer (DMO) during surface intervals, immediately following the final  
225 decompression, 2 hours post-dive, and the day after the dive. All technical reports by the DCIEM [24-29]  
226 used the following onset time determination procedure: divers were monitored with a Doppler Prechordal  
227 Bubble Detector, both at rest and while exercising during the dive, and then at 30-minute intervals for at  
228 least 1.5-3 hours post-dive. If a diver's Doppler bubble score was still elevated at this time, he/she  
229 remained under medical surveillance until this score decreased. A diver's account of symptoms was used  
230 to determine the onset time of DCS by a medical officer.

231 The occurrence density function for the entire BIG292 data set, excluding marginal DCS cases, is  
232 shown in Figure 1. The time scale of the ODF ranges from mid-dive (indicated by negative values for time)  
233 to post-dive (indicated by positive values for time) with 0 hours representing the completion of  
234 decompression. The first peak of this bimodal plot occurs at 0 hours after decompression and the second  
235 peak occurs at 2 hours after decompression. A trace of the computational model LE1-USN93  
236 parameterized without marginal DCS events [15] is also represented in Figure 1. Note that the LE1-USN93  
237 ODF is not bimodal, with a peak at 0 hours after the final decompression.

238 The ODF of marginal DCS cases is plotted in Figure 2. This plot contains a trace for all 110 marginal  
239 DCS cases (both with and without onset times), and a trace for the 68 marginal DCS cases with onset times.  
240 Both ODFs are unimodal with both peaks occurring at 1 hour after the final decompression. This unimodal  
241 marginal DCS data is excluded from all further ODF analysis in this work.

242 DCS onset times  $T_1$  and  $T_2$  are ranked and plotted in Figure 3. DCS occurrences were sorted first  
243 by  $T_1$ , indicated by the leftmost solid line. DCS occurrences that share the same  $T_1$  were then sorted by  
244  $T_2$ , as indicated by the rightmost line. The gray shaded region indicates the time between  $T_1$  and  $T_2$ . This  
245 plot serves to graphically display the disparity in the symptom event window duration. The DCS events  
246 contributing to the first and second peaks are indicated in the figure. Despite this disparity in event  
247 window, there is no obvious indication in the figure of what causes the bimodal peak.

248 Histograms displaying the distributions of  $T_1$  and  $T_2$  can be found in Figure 4. The leftmost and  
249 rightmost bars in both histograms include all onset times before 6 hours prior to surfacing and after 6  
250 hours post-dive respectively. The frequency of  $T_1$  times peaks at 2 hours post-dive, with only one case  
251 having  $T_1$  exceed 2 hours (by 1 minute). The frequency of  $T_2$  times peaks immediately after surfacing  
252 and again after 2 hours post-dive, then a significant portion of  $T_2$  times are after 6 hours post-dive.

### 253 Dive type

254 DCS occurrence density functions were generated for each of the five dive type and breathing gas  
255 combinations included in the BIG292 dive data set, excluding marginal DCS outcomes (Figure 5). The  
256 individual data files corresponding to each dive type and the shapes of the resulting ODF (bimodal,  
257 unimodal, or ambiguous) are reported in Table 2. The single air, single non-air, repetitive and multi-level  
258 air, and repetitive and multi-level non-air ODFs have a bimodal shape. The first peak of all these plots  
259 occurs at 0 hours and the second peak occurs at 2 hours after the final decompression. Though these dive  
260 types differ in numbers of DCS occurrences, the timing of the peaks is consistent across dive type. The  
261 saturation dive ODF is ambiguous in shape, with a peak at 0 hours after decompression and a sharp decline  
262 in DCS occurrence after 2 hours. Unlike the bounce dives, saturation diving displays a substantial  
263 frequency of DCS onset during decompression (prior to surfacing). However, this dive type difference  
264 does not affect the bimodality of the BIG292 ODF.

## 265 Event Severity

266 Separate ODFs were generated for mild DCS and serious DCS cases, using both Type I/II and Type  
267 A/B data splitting and excluding marginal DCS cases. The distribution of PSI classifications into each  
268 splitting method is reported in Table 3, along with the number of DCS events in each mild or severe  
269 categorization and the shapes of the resulting ODFs. All plots are bimodal, with the first peak at 0 hours  
270 and the second peak at 2 hours after the final surface interval (Figure 6).

## 271 Symptom Type

272 The shape of the ODF for each PSI is reported in Table 4. The ODFs for pain and serious  
273 neurological symptoms are bimodal, with the first peak at 0 hours and the second peak at 2 hours after  
274 the final decompression. The ODFs for constitutional, skin, mild neurological, and cardiopulmonary  
275 symptoms are ambiguously shaped, likely due to the low number of DCS events with these symptom types  
276 in the BIG292 data.

## 277 Institution

278 ODFs were generated for each individual dive report contained in the BIG292 data set, then ODFs  
279 were created for all the dive reports published by each institution (Table 5). The NEDU 11-80 [30], NEDU  
280 1-84 [31], and NSMRL 1200 [21] technical reports each generated ambiguously shaped ODFs, likely due to  
281 the low number of DCS events in each report. The NEDU 8-85 [32], NEDU 1-99/NMRC 99-01 [22], NMRI  
282 86-97 [23], and all DCIEM technical reports (DCIEM 80-R-32 [29], DCIEM 81-R-02 [27], DCIEM 82-R-38 [28],  
283 DCIEM 84-R-72 [24], DCIEM 84-R-73 [25], DCIEM 85-R-18 [26]) each yielded bimodal ODFs. All bimodal  
284 ODFs had a first peak at 0 hours and a second peak at 2 hours after final decompression. All ambiguously  
285 shaped ODFs had a peak at 0 hours after the final decompression. However, by inspection of the  $T_1$  and  
286  $T_2$  times corresponding to the ambiguous ODFs, these DCS event windows are consistent with those  
287 generating bimodal ODFs. Regardless of onset time measurement procedure, ODFs for all reports were

288 either bimodal (with the first peak at 0 hours and second peak at 2 hours after the final decompression)  
289 or ambiguously shaped; the latter likely due to insufficient quantity of DCS events documented by that  
290 particular dive report.

291 Saturation dive data were not partitioned by report or institution. The four saturation dive files  
292 (ASATARE, ASATNSM, ASATEDU, ASATNMR) contain data from 30 reports and dive test plans with  
293 publication spanning 1979-1992 [2, 3]. The removal of saturation dive data does not affect the bimodality  
294 of the ODFs of other dive types as many resulting DCS events occurred prior to surfacing (Figure 5), so  
295 further partitioning by dive report was not warranted.

## 296 Chronology of Dive Trials

297 ODFs were generated for dive trials completed during 1978-1983, 1984, 1985-1987, and 1988-  
298 1992 (Table 6). These temporal groupings were selected to each include similar quantities of DCS events.  
299 The ODFs for 1984, 1985-1987, and 1988-1992 are bimodal, with the first peak at 0 hours and the second  
300 peak at 2 hours following decompression. The ODF for dive trials completed during 1978-1983 is  
301 unimodal, with a peak at 0 hours after the final decompression (Figure 7).

## 302 Discussion

303 The goal of this work was to determine the cause of the bimodality in the BIG292 ODF to enable  
304 replication of this bimodal behavior in probabilistic models of DCS. The source of the bimodality would  
305 be revealed if a particular data partitioning method resulted in a set of unimodal ODFs, some peaking at  
306 0 hours and others at 2 hours following decompression. All but one iteration of data partitioning resulted  
307 in a bimodal or ambiguously shaped ODF; the latter likely due to an insufficient quantity of DCS events in  
308 that group.

309            Partitioning the data by dive type, DCS severity, DCS symptom type, or institution did not provide  
310 any insight into the source of the bimodal peak. The ODFs for single air, single non-air, repetitive and  
311 multi-level air, and repetitive and multi-level non-air dives were all bimodal. The ODF for saturation dives  
312 had only one peak, which occurred at 0 hours after decompression, but followed a bimodal shape, with a  
313 sharp decline in DCS occurrences after 2 hours post-dive. No dive type could be identified as the source  
314 of either of the bimodal peaks. When analyzing Type I/II and Type A/B data splitting, the ODFs for all mild  
315 and severe categorizations were bimodal. Further, ODFs for each PSI with a sufficient number of DCS  
316 occurrences were bimodal. Therefore, the second peak in the BIG292 bimodal ODF cannot be attributed  
317 to a discrepancy in DCS onset time based on DCS symptom severity or type. Similarly, splitting the dive  
318 data based on the institution that conducted the dive trials, and further by each report published,  
319 generated either bimodal or ambiguously shaped ODFs; the latter likely due to an insufficient quantity of  
320 DCS occurrences in that data set to produce a typical ODF. Thus, slight institutional differences in dive  
321 trial protocol are not responsible for the bimodality of the BIG292 ODF.

322            DCS occurrence data from dive trials completed during 1978-1983 produced a unimodal ODF. In  
323 all dive trial reports pertaining to the BIG292 data set except the NEDU technical reports 11-80, 1-84, and  
324 8-85, a strict onset time measurement protocol was established, in which all divers were examined by a  
325 DMO immediately after surfacing, and then again after 2 hours. NEDU technical reports 11-80, 1-84, and  
326 8-85 do not explicitly document that divers were examined at 2 hours post-dive, although the NEDU 11-  
327 80 does indicate that divers were released from the hyperbaric chamber facility at this 2-hour mark. Thus,  
328 dive data produced by the NEDU during the 1978-1983 trial end date range may not have used the above  
329 onset time determination protocol. In addition, one reviewer pointed out that the decompression  
330 schedules tested during this early date range were riskier, thus the onset of DCS events in these trials  
331 occurred during decompression or shortly thereafter. Many of the  $T_2$  times reported in these trials are  
332 within 2 hours of decompression, and divers were under medical surveillance during this time. Thus, the

333 corresponding onset time windows are smaller and the ODF is unimodal. As decompression schedules  
334 improved, divers were able to surface without incident but experienced DCS onset after surfacing. In  
335 these later trials, divers were monitored by a DMO for 2 hours (NEDU, NMRC, NSMRL) or 1.5-3 hours  
336 (DCIEM) before being released if no symptoms developed. For many DCS cases with onset after this  
337 window of post-dive medical surveillance, the  $T_1$  time is 2 hours, which is when close medical examination  
338 of the diver ended (and corresponds to the second ODF peak). This bias towards a  $T_1$  time of 2 hours with  
339 delayed-onset DCS is apparent in Figure 4, as the  $T_1$  histogram contains a peak in the bin range (1,2]. Only  
340 one DCS case in the BIG292 data set has a  $T_1$  time greater than 2 hours, and this onset time is 2 hours and  
341 1 minute. In Figure 3, DCS events with  $T_1=0$  hours generally correspond to short event windows, while  
342 those with  $T_2=2$  hours arise from delayed DCS onset (as indicated by the large shaded region). This is  
343 consistent with our conclusion that the  $T_1$  for delayed DCS onset cases was biased towards  $T_1=2$  hours.  
344 These long windows are a result of termination of continuous medical surveillance at 2 hours post-dive,  
345 thus the last known time a diver was definitely asymptomatic was set as  $T_1=2$  hours if symptoms  
346 developed after this time.

347         The bimodal shape of the BIG292 ODF is likely due to the medical surveillance protocol used in  
348 determining the onset time of DCS symptoms. It may be possible to eliminate this bimodality in future  
349 dive trial data if medical examination of divers is scheduled more frequently in the 24 hours following  
350 decompression. If divers were to be examined more often between 2 hours and 24 hours post-dive, there  
351 would be a lower number of  $T_1=2$  hours cases, as  $T_1$  would now reflect these later examination times. This  
352 could aid in shortening the event window, as  $T_1$  and  $T_2$  times would become more accurate.

353         Although computational replication of the bimodal shape of the BIG292 ODF would increase the  
354 likelihood, implying a better fit of the model to the data, doing so would be meaningless because there is  
355 not a distinct source (differences in dive type or DCS event severity) of the second peak. The single peak  
356 produced by current models of DCS which merges the bimodal peaks of the data in the ODF is very likely



357 the correct solution. The ODF is still however a valuable tool for assessing the performance of models  
358 which predict the onset time of DCS. ODFs provide a qualitative metric to confirm that the onset time is  
359 being correctly predicted by the underlying model.

## 360 Conclusions

361 We investigated the potential sources of the bimodal shape of the BIG292 ODF with the goal of  
362 identifying features in the DCS cases that could potentially lead to an improvement in DCS model  
363 prediction. We found that bimodal shape of ODFs of DCS occurrences in empirical dive data were not  
364 related to dive types, severity of DCS symptoms, or symptom type. The DCS onset time determination  
365 protocol used by each institution that contributed human dive trial data to the U.S. Navy collection that  
366 became the BIG292 collection was reviewed. The common protocol between all institutions involved  
367 examination by a medical officer immediately after decompression and again in approximately 2 hours.  
368 The unimodal ODF corresponding to dive data from 1978-1983 is likely due to the higher risk  
369 decompression schedules that were tested during these trials, thus DCS onset occurred during  
370 decompression or shortly thereafter. In later trials with less risky decompression schedules (post-1984),  
371 DCS onset tended to occur after the 2-hour window of close medical surveillance. We conclude that the  
372 bimodality of the BIG292 ODF is likely due to a combination of delayed DCS onset in post-1984 trials, as  
373 decompression schedules became safer, and the protocol for determining DCS symptom onset time, in  
374 which divers were released from medical officer surveillance if no symptoms developed around 2 hours  
375 post-dive. When the time of symptom onset information is used in optimizing probabilistic DCS models,  
376 the log likelihood function implicitly aligns the model's ODF prediction with that of the calibration data.  
377 Thus, if a model were able to replicate the data's bimodal ODF, the model would generate a greater log  
378 likelihood than a model which generated a unimodal ODF. This would lead one to conclude that the model  
379 replicating the bimodal ODF were the better of the two models. However, replicating the bimodal ODF

380 shape in probabilistic models would likely be meaningless; as the ODF bimodality is not caused by dive  
381 type, DCS event severity, or symptom type but is rather related to the DCS onset time measurement  
382 protocol.

## 383 Acknowledgements

384 We would like to thank Dr. David Doolette of the Navy Experimental Unit for his helpful discussion related  
385 to this work. We would also like to thank the five anonymous reviewers for their many helpful comments  
386 and suggestions. This work was supported by Naval Sea Systems Command (NAVSEA-00C -  
387 <http://www.navsea.navy.mil/>) under contracts N00024-13-C-4104 and N00024-17-C4317 and the Office  
388 of Naval Research under grant N000141310063. BelleQuant Engineering, PLLC provided computational  
389 resources. Neither the funding agency nor the commercial entity played any role in designing this study,  
390 data collection and analysis, decision to publish, interpreting the results, or writing the manuscript.

## 391 Bibliography

- 392 [1] R.E. Moon, R.D. Vann, P.B. Bennett, The Physiology of Decompression Illness, *Scientific American*,  
393 273 (1995) 54-61.
- 394 [2] D.J. Temple, R. Ball, P.K. Weathersby, E.C. Parker, S.S. Survanshi, The Dive Profiles and Manifestations  
395 of Decompression Sickness Cases After Air and Nitrogen-Oxygen Dives. Volume I: Data Set Summaries,  
396 Manifestation Descriptions, and Key Files. NMRC 99-02(Vol. I), Naval Medical Research Center,  
397 Bethesda, MD, 1999.
- 398 [3] D.J. Temple, R. Ball, P.K. Weathersby, E.C. Parker, S.S. Survanshi, The Dive Profiles and Manifestations  
399 of Decompression Sickness Cases After Air and Nitrogen-Oxygen Dives. Volume II: Complete Profiles and  
400 Graphic Representations for DCS Events. NMRC 99-02(Vol II.), Naval Medical Research Center, Bethesda,  
401 MD, 1999.
- 402 [4] A.E. Boycott, G.C.C. Damant, J.S. Haldane, The prevention of compressed-air illness, *Journal of*  
403 *Hygiene*, 8 (1908) 342-443.
- 404 [5] T.E. Berghage, J.M. Woolley, L.J. Keating, The probabilistic nature of decompression sickness,  
405 *Undersea Biomedical Research*, 1 (1974) 189-196.
- 406 [6] P.K. Weathersby, L.D. Homer, E.T. Flynn, On the likelihood of decompression sickness, *Journal of*  
407 *Applied Physiology: Respiration Environmental Exercise Physiology*, 57 (1984) 815-825.
- 408 [7] P.K. Weathersby, W.A. Gerth, Survival analysis and maximum likelihood techniques as applied to  
409 physiological modeling, in: P.K. Weathersby, W.A. Gerth (Eds.) *Fifty-first Workshop of the Undersea and*  
410 *Hyperbaric Medical Society*, Undersea and Hyperbaric Medical Society, 2002.
- 411 [8] P.K. Weathersby, S.S. Survanshi, L.D. Homer, E. Parker, E.D. Thalmann, Predicting the time of  
412 occurrence of decompression sickness, *Journal of Applied Physiology*, 72 (1992) 1541-1548.

413 [9] E.C. Parker, S.S. Survanshi, P.K. Weathersby, Improving on a "Good" Model, in: P.K. Weathersby,  
414 W.A. Gerth (Eds.) Fifty-first Workshop of the Undersea and Hyperbaric Medical Society, Undersea and  
415 Hyperbaric Medical Society, 2002, pp. 137-141.

416 [10] E.D. Thalmann, E.C. Parker, S.S. Survanshi, P.K. Weathersby, Improved probabilistic decompression  
417 model risk predictions using linear-exponential kinetics, Undersea and Hyperbaric Medical Society, 24  
418 (1997) 255-274.

419 [11] W.A. Gerth, R.D. Vann, Probabilistic gas and bubble dynamics models of decompression sickness  
420 occurrence in air and nitrogen-oxygen diving, Undersea and Hyperbaric Medical Society, 24 (1997) 275-  
421 292.

422 [12] E.A. Hada, On the advancement of probabilistic models of decompression sickness (Doctoral  
423 Dissertation), Department of Mechanical Engineering and Materials Science, Duke University, Durham,  
424 NC, 2016, pp. 136.

425 [13] F.G. Murphy, E.A. Hada, D.J. Doolette, L.E. Howle, Probabilistic pharmacokinetic models of  
426 decompression sickness in humans, part 1: Coupled perfusion-limited compartments, Computers in  
427 Biology and Medicine, 86 (2017) 55-64.

428 [14] L.E. Howle, P.W. Weber, R.D. Vann, M.C. Campbell, Marginal DCS events: their relation to  
429 decompression and use in DCS models, Journal of Applied Physiology, 107 (2009) 1539-1547.

430 [15] F.G. Murphy, The impact of weighting marginal DCS events as non-events, pharmacokinetic gas  
431 content models, and optimal decompression schedule calculation (Doctoral Dissertation), Mechanical  
432 Engineering and Materials Science, Duke University, Durham, NC, 2017, pp. 194.

433 [16] R.D. Vann, P.J. Denoble, L.E. Howle, P.W. Weber, J.J. Freiburger, C.F. Pieper, Resolution and Severity  
434 in Decompression Illness, Aviation, Space, and Environmental Medicine, 80 (2009) 466-471.

435 [17] L.E. Howle, P.W. Weber, E.A. Hada, R.D. Vann, P.J. Denoble, The probability and severity of  
436 decompression sickness, PLOS ONE, 12 (2017) e0172665.

437 [18] L.E. Howle, P.W. Weber, J.M. Nichols, Bayesian approach to decompression sickness model  
438 parameter estimation, Computers in Biology and Medicine, 82 (2017) 3-11.

439 [19] W.H. Press, S.A. Teukolsky, W.T. Vetterling, B.P. Flannery, Numerical Recipes in C: The Art of  
440 Scientific Computing, 2nd ed., Cambridge University Press, Cambridge, UK, 1992.

441 [20] E.C. Parker, S.S. Survanshi, P.B. Massell, P.K. Weathersby, Probabilistic models of the role of oxygen  
442 in human decompression sickness, Journal of Applied Physiology, 84 (1998) 1096-1102.

443 [21] C.L. Shake, P.K. Weathersby, D. Wray, E.C. Parker, Decompression Sickness Resulting from Long  
444 Shallow Air Dives. NSMRL 1200, Naval Submarine Medical Research Laboratory, 1996.

445 [22] E.D. Thalmann, P.C. Kelleher, S.S. Survanshi, E.C. Parker, P.K. Weathersby, Statistically Based  
446 Decompression Tables XI: Manned Validation of the LE Probabilistic Model for Air and Nitrogen-Oxygen  
447 Diving. NMRI 99-01/NEDU TR 1-99, Joint Technical Report: Naval Medical Research Center and Navy  
448 Experimental Diving Unit, Bethesda, MD, 1999.

449 [23] P.K. Weathersby, B.L. Hart, E.T. Flynn, W.F. Walker, Human Decompression Trial in Nitrogen-Oxygen  
450 Diving. NMRI 86-97, Naval Medical Research Institute, Bethesda, MD, 1986.

451 [24] G.R. Lauckner, R.Y. Nishi, B.C. Eatock, Evaluation of the DCIEM 1983 Model for Compressed Air  
452 Diving (Series A-F). DCIEM 84-R-72, Defence and Civil Institute of Environmental Medicine, Downsview,  
453 ON, 1984.

454 [25] G.R. Lauckner, R.Y. Nishi, B.C. Eatock, Evaluation of the DCIEM 1983 Model for Compressed Air  
455 Diving (Series G-K). DCIEM 84-R-73, Defence and Civil Institute of Environmental Medicine, Downsview,  
456 ON, 1984.

457 [26] G.R. Lauckner, R.Y. Nishi, B.C. Eatock, Evaluation of the DCIEM 1983 Model for Compressed Air  
458 Diving (Series L-Q). DCIEM 85-R-18, Defence and Civil Institute of Environmental Medicine, Downsview,  
459 ON, 1985.

460 [27] R.Y. Nishi, B.C. Eatock, I.P. Buckingham, G. Masurel, XDC-2 Digital Decompression Computer:  
461 Assessment of Decompression Profiles by Ultrasonic Monitoring, Phase II: 30-75 msw. DCIEM 81-R-02,  
462 Defence and Civil Institute of Environmental Medicine, Downsview, ON, 1981.  
463 [28] R.Y. Nishi, B.C. Eatock, I.P. Buckingham, B.A. Ridgewell, Assessment of Decompression Profiles by  
464 Ultrasonic Monitoring, Phase III: No-Decompression Dives. DCIEM 82-R-38, Defence and Civil Institute of  
465 Environmental Medicine, Downsview, ON, 1982.  
466 [29] R.Y. Nishi, K.E. Kisman, I.P. Buckingham, B.C. Eatock, G. Masurel, XDC-2 Digital Decompression  
467 Computer: Assessment of Decompression Profiles by Ultrasonic Monitoring, Phase I: 36-54 msw. DCIEM  
468 80-R-32, Defence and Civil Institute of Environmental Medicine, Downsview, ON, 1980.  
469 [30] E.D. Thalmann, I.P. Buckingham, W.H. Spaur, Testing of Decompression Algorithms for Use in the U.  
470 S. Navy Underwater Decompression Computer. Phase I. NEDU TR 11-80, Navy Experimental Diving Unit,  
471 Panama City, FL, 1980.  
472 [31] E.D. Thalmann, Phase II Testing of Decompression Algorithms for Use in the U.S. Navy Underwater  
473 Decompression Computer. NEDU TR 1-84, Navy Experimental Diving Unit, Panama City, FL, 1984.  
474 [32] E.D. Thalmann, Air-N<sub>2</sub>O<sub>2</sub> Decompression Computer Algorithm Development. NEDU TR 8-85, Navy  
475 Experimental Diving Unit, Panama City, FL, 1986.

476

477

Report Contributing to the BIG292 Data Set	DCS Onset Time Measurement Method
NEDU 11-80 [30]	Following decompression, divers remained at the dive chamber for 2 hours then were required to be within 30 min of facility for the next 4 hours. The dive chamber facility was prepared to provide DCS treatment for 24 hours post-dive.
NEDU 1-84 [31]	A US Navy Diving Medical Officer (DMO) examined all divers after surfacing.
NEDU 8-85 [32]	Divers could report symptoms of DCS at all times, including during the dive. All DCS determination was made by a DMO.
NEDU 1-99 / NMRC 99-01 [22]	Divers were examined by a DMO during surface intervals (for repetitive dives) and immediately after completing each dive. If no DCS symptoms were present, divers were re-examined 2 hours later. Divers were required to be in the presence of someone who could recognize DCS for the next 24 hours. The DMO then re-examined each diver the next morning after their dive.
NMRI 86-97 [23]	Divers were examined by a DMO upon completion of the dive and again after 2 hours following decompression. Divers could report symptoms for 18 hours post-dive and were interviewed by a DMO the morning after the dive.
NSMRL 1200 [21]	The DMO examined divers immediately post-dive, 2 hours post-dive, and 24 hours post-dive. Divers could report symptoms at any time.
DCIEM 80-R-32 [29]	Divers were monitored with Doppler Prechordal Bubble Detector, both at rest and after performing an exercise during the dive. Divers were monitored with this device pre-dive, at 15 min intervals during the dive, immediately post-dive, and periodically for at least 3 hours post-dive. Divers could report symptoms at any time. The decision to treat for DCS was not based on doppler results, however these results were used by the DMO to determine if diver symptoms required recompression.
DCIEM 81-R-02 [27]	Divers were monitored with Doppler Prechordal Bubble Detector, both at rest and after performing an exercise during the dive. Divers were monitored with this device pre-dive, at 15 min intervals during the dive, immediately post-dive, and periodically for at least 3 hours post-dive. Divers could report symptoms at any time.

DCIEM 82-R-38 [28]	Divers were monitored with Doppler Prechordal Bubble Detector, both at rest and after performing an exercise during the dive. Divers remained at rest for 90 min post-dive. Divers could report symptoms at any time.
DCIEM 84-R-72 [24]	Divers were monitored with the Doppler Bubble Detector before each dive, and at 30 min intervals for at least 2 hours post-dive while resting. If bubbles were detected, the diver remained under observation until bubbles diminished. Divers could report symptoms at any time. The DMO determined treatment based on symptoms, not bubble grades.
DCIEM 84-R-73 [25]	Divers were monitored with the Doppler Bubble Detector before each dive, and at 30 min intervals for at least 2 hours post-dive while resting. If bubbles were detected, the diver remained under observation until bubbles diminished. Divers could report symptoms at any time. The DMO determined treatment based on symptoms, not bubble grades.
DCIEM 85-R-18 [26]	Divers were monitored with the Doppler Bubble Detector before each dive, and at 30 min intervals for at least 2 hours post-dive while resting. If bubbles were detected, the diver remained under observation until bubbles diminished. Divers could report symptoms at any time. The DMO determined treatment based on symptoms, not bubble grades.

Table 1. DCS onset time measurement method of dive reports in the BIG292 data set. The NEDU 1-99 / NMRC 99-01 and NSMRL 1200 followed a consistent method of examining divers immediately post-dive, 2 hours post-dive, and the day after the dive. All DCIEM reports followed a similar procedure of monitoring divers during the dive and for 1.5-3 hours post-dive. The NEDU reports 11-80, 1-84, and 8-85 do not explicitly document that divers were examined at 2 hours post-dive, although the NEDU 11-80 does indicate that divers were released from the hyperbaric chamber facility at this 2-hour mark.

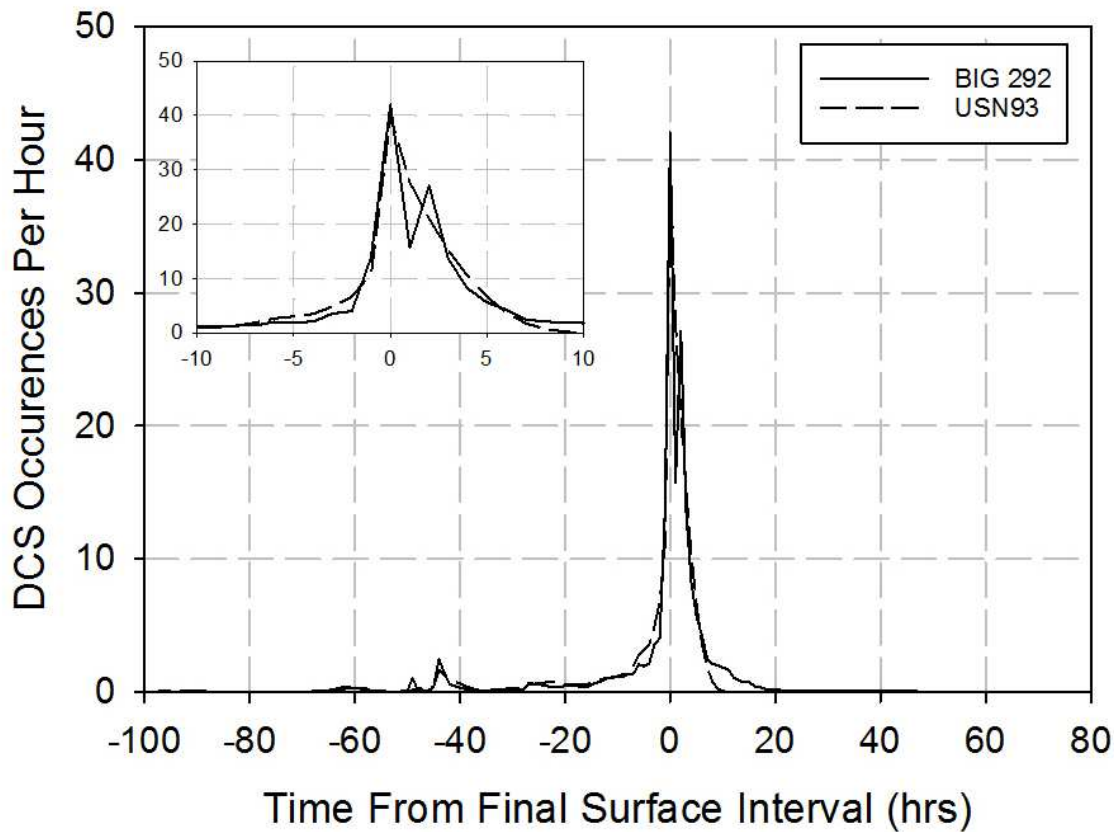


Figure 1. Occurrence density function of the BIG292 data set and predictions from the LE1-USN93 computational model, excluding marginal DCS cases [15]. The ODF is a plot of the number of DCS occurrences per hour relative to the final surface time. Time less than zero indicates that the onset of DCS occurred before the completion of the dive. This plot is bimodal, with one peak at 0 hours and a second peak at 2 hours after the final surface time. The bimodality is not dependent on the presence or absence of marginal DCS cases. The dashed line shows the prediction from the LE1-USN93 computational model (recalibrated without marginal DCS events [15]). The ODF produced by this model is not bimodal. The magnified view of the ODF in the top left more clearly illustrates the bimodal behavior of the onset of DCS symptoms in dive trial data.

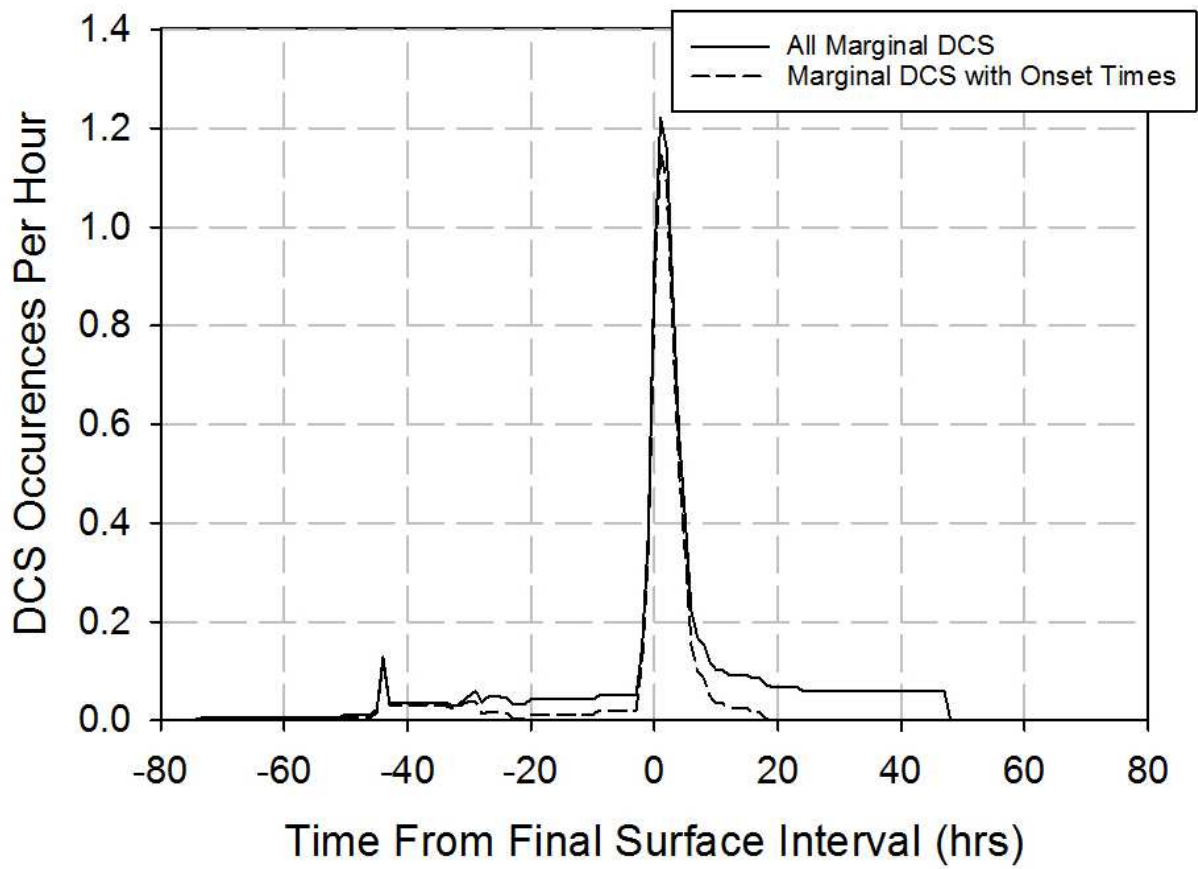


Figure 2. Occurrence density functions for marginal DCS cases. The solid line trace includes data for all 110 marginal DCS cases in the BIG 292 data set, and the dashed line trace plots only marginal DCS cases with recorded onset times (68 cases). Both ODFs are unimodal, with both peaks at 1 hour after the final surface time.



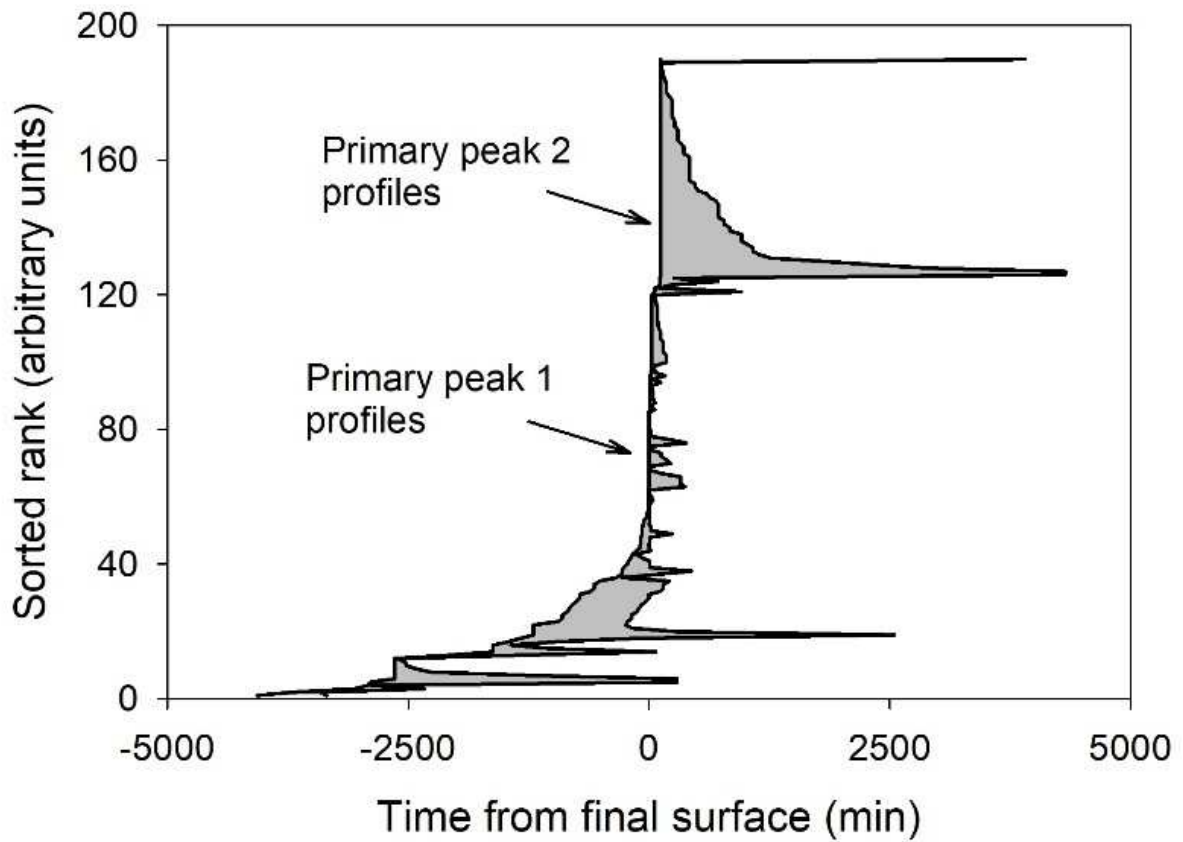


Figure 3. DCS onset time  $T_1$  and  $T_2$  ranking.  $T_1$  is the last known time a diver was symptom free, and  $T_2$  is the earliest time the diver was definitely experiencing symptoms. DCS occurrences were sorted first by  $T_1$ , indicated by the leftmost line. DCS occurrences that share the same  $T_1$  were then sorted by  $T_2$ , as indicated by the rightmost line. The shaded region shows the timespan between  $T_1$  and  $T_2$ . This plot serves to graphically display the disparity in the symptom event window size. The profiles primarily contributing to the first and second ODF peaks are indicated, as the two long vertical segments correspond to 0 and 2 hours. DCS events with  $T_1=0$  hours generally correspond to short event windows, while those with  $T_2=2$  hours are consistent with delayed DCS onset (as indicated by the large shaded region).

485

486

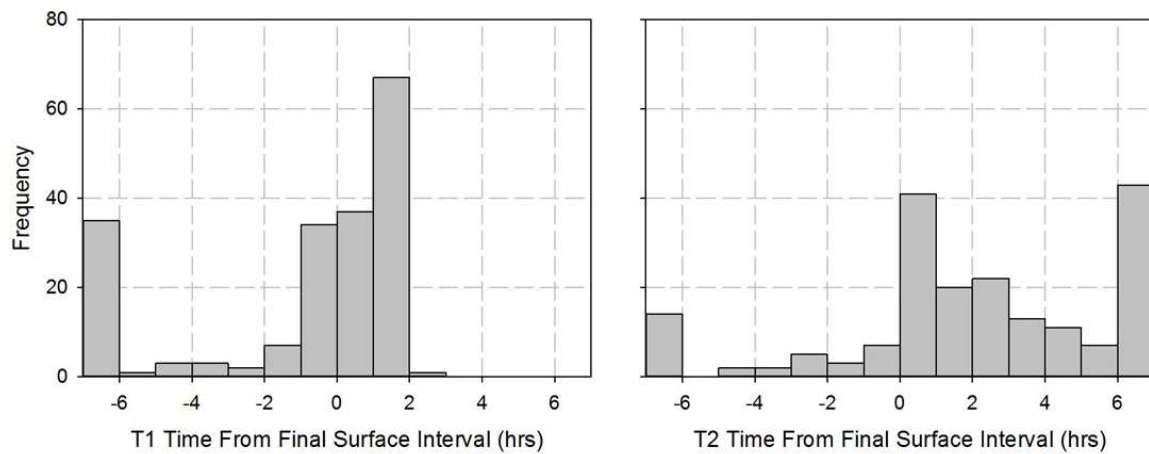


Figure 4. Distributions of  $T_1$  and  $T_2$  times of the DCS events in the BIG292 data set. Time less than zero indicates that the onset of DCS occurred before the completion of the dive. The leftmost and rightmost bars include all onset times prior to -6 hours and after 6 hours relative to surfacing respectively. The most frequent  $T_1$  time is 2 hours post-dive (as indicated by the peak frequency in the (1,2] bin range), with the only  $T_1$  time exceeding 2 hours being 2 hours and 1 minute. Many of the  $T_1$  times prior to -6 hours correspond to saturation diving (see Figure 4). The peak in  $T_2$  times during (0,1] hour post-dive relate to DCS events with rapid onset and correspond to  $T_1$  times during decompression. The significant quantity of  $T_2$  times after 6 hours post-dive indicates delayed symptom onset; many of these late  $T_2$ 's correspond to  $T_1$  at 2 hours.

Dive Type	BIG292 Files	Number of DCS Occurrences (excluding marginal DCS cases)	ODF Shape
Single Air	EDU885A	53	Bimodal
	DC4W		
	SUBX87		
	NMRNSW		
	PASA		
	NSM6HR		
Repetitive and Multi-level Air	EDU885AR	34	Bimodal
	DC4WR		
	PARA		
	PAMLA		
Single Non-air	NMR8697	25	Bimodal
	EDU885M		
	EDU1180S		
Repetitive and Multi-level Non-air	EDU184	26	Bimodal
	PAMLAOD		
	PAMLAOS		
	EDU885S		
Saturation	ASATEDU	52	Ambiguous
	ASATNMR		
	ASATNSM		
	ASATARE		

Table 2. Data partitioned by dive type. The data files in the BIG292 data set were categorized by dive type and ODFs were generated for each grouping (Figure 5), excluding marginal DCS cases. All ODFs were bimodal except for that of the saturation dives, which was ambiguous in shape. All bimodal plots had the first peak at 0 hours and the second peak at 2 hours following decompression.

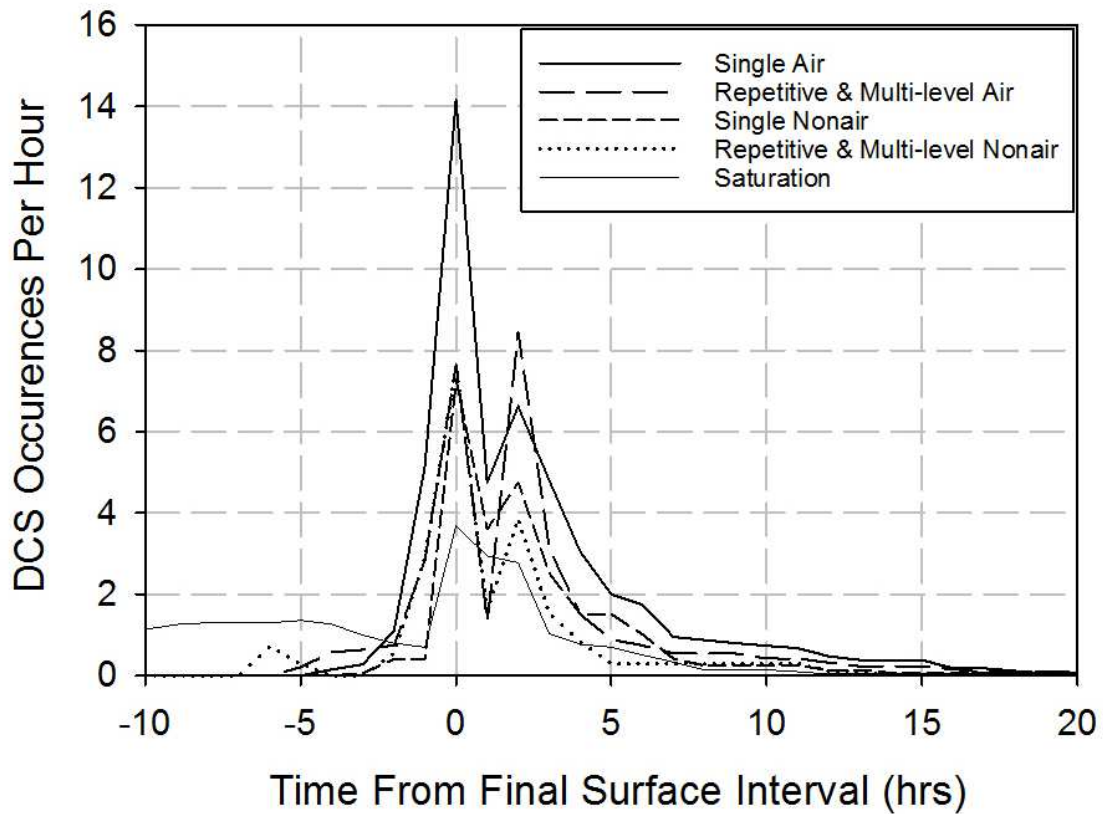


Figure 5. Occurrence density functions for the BIG292 data set partitioned by dive type. See Table 2 for the categorization of the BIG292 data files. The ODFs for all dive types except saturation dives are bimodal, with the first peak at 0 hours and the second peak at 2 hours after the final decompression. Unlike the bounce dives, saturation diving displays a substantial frequency of DCS onset during decompression (prior to surfacing). However, this dive type difference does not affect the bimodality of the BIG292 ODF.

489

490

491

Perceived Severity Index	Type I/II	Type A/B
Constitutional	Type I 152 DCS Occurrences Bimodal	Type A 170 DCS Occurrences Bimodal
Skin		
Pain		
Mild Neurological	Type II 38 DCS Occurrences Bimodal	Type B 20 DCS Occurrences Bimodal
Cardiopulmonary		
Serious Neurological		

Table 3. Data partitioned by event severity (Type I/II and Type A/B classifications) [17]. Each DCS case in the BIG292 data set was assigned a PSI value based on the reported symptoms. These cases were then categorized into Type I or Type II, then Type A or Type B, by their PSI. Type I and Type A are considered mild cases of DCS, while Type II and Type B are serious cases. ODFs were generated for Type I, Type II, Type A, and Type B DCS cases, excluding marginal DCS cases (Figure 6). All plots were bimodal, with the first and second peaks occurring at 0 and 2 hours after the final decompression, respectively.

492

493

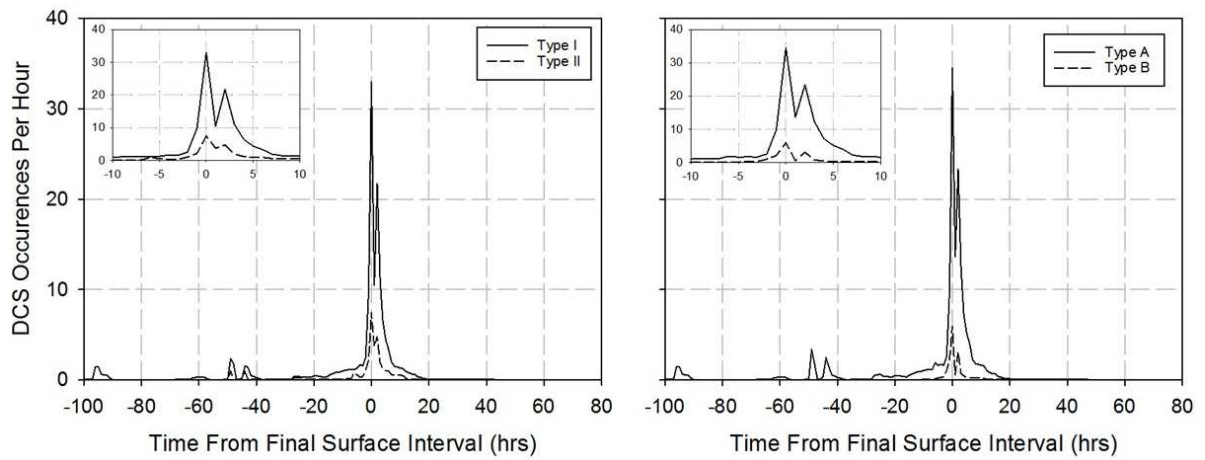


Figure 6. Occurrence density functions for the BIG292 data set partitioned by event severity (Type I/II and Type A/B classifications). See Table 3 for categorization by PSI. All ODFs are bimodal, with the first peak at 0 hours and the second peak at 2 hours after the final decompression. The magnified views of each ODF in the top left corners more clearly illustrate the bimodal behavior of DCS symptom onset time.

494

495

496

Symptom Type	Number of DCS Occurrences (excluding marginal DCS cases)	ODF Shape Based on Symptom Type
Constitutional	1	Insufficient data
Skin	1	Insufficient data
Pain	149	Bimodal
Mild Neuro	18	Insufficient data
Cardio	2	Insufficient data
Serious Neuro	18	Bimodal

Table 4. Data partitioned by symptom type. Each DCS case in the BIG292 data set was assigned a PSI value based on the reported symptoms, and ODFs were generated for each symptom type. The ODFs for pain and serious neurological symptoms were bimodal. The first and second peaks occurred at 0 hours and 2 hours after the final surface interval, respectively. ODFs for other symptom types did not have enough exposures to produce non-ambiguously-shaped plots.

497

498

Institution	Report	Files	Number of DCS Occurrences (excluding marginal DCS cases)	ODF Shape Based on Report	ODF Shape Based on Institution
NEDU	NEDU 11-80 [30]	EDU1180S	10	Insufficient data	Bimodal
	NEDU 1-84 [31]	EDU184	11	Insufficient data	
	NEDU 8-85 [32]	EDU885A	49	Bimodal	
		EDU885AR			
		EDU885M			
		EDU885S			
	NEDU 1-99 <sup>l</sup> [22]	PASA	36	Bimodal	
		PAMLA			
		PARA			
		PAMLAOS			
PAMLAOD					
NMRC	NMRI 86-97 [23]	NMR8697	11	Bimodal	Bimodal
	NMRI Protocol 88-06 (no report published)	NMRNSW	5	Insufficient data	
	NMRC 99-02 <sup>ll</sup> [2, 3]	ASATEDU	52	Ambiguous	
		ASATNMR			
		ASATNSM			
		ASATARE			
	NMRC 99-01 <sup>l</sup> [22]	PASA	36	Bimodal	
		PAMLA			
		PARA			
		PAMLAOS			
PAMLAOD					
NSMRL	NSMRL 1200 [21]	NSM6HR	3	Insufficient data	Ambiguous
DCIEM	Several [24-29]	DC4W	11	Bimodal	Bimodal
		DC4WR			

<sup>l</sup> The four saturation dive files (ASATARE, ASATNSM, ASATEDU, ASATNMR) contain data from 30 reports and dive test plans with publication spanning 1979-1992. For brevity, Temple *et al.* is cited for these files.

<sup>ll</sup>T NEDU 1-99 and NMRC 99-01 was a joint report between the Navy Experimental Diving Unit and the Naval Medical Research Center. This report was grouped with both institutions.



INM	No report published	SUBX87	2	Insufficient data	Ambiguous
-----	---------------------	--------	---	-------------------	-----------

Table 5. Data partitioned by institution. The data files in the BIG292 data set were categorized by the institution conducting the dive trial. ODFs were generated separately for each dive report, and then for all the reports published by each institution. All marginal DCS cases were excluded. The first column indicates the institution (Navy Experimental Diving Unit, Naval Medicine Research Center, Naval Submarine Medical Research Laboratory, Defense and Civil Institute of Environmental Medicine, Institute of Naval Medicine) that conducted the dive trials. The second column includes each dive report published by that institution, and the third column indicates the dive files in the BIG292 data set that were described by each report. Columns four and five show the number of DCS occurrences in each dive file and the shape of the ODF for those exposures, respectively. The sixth column indicates the ODF shape for all the dive data from each institution. The NEDU 11-80, NEDU 1-84, NMRI 88-06, NSMRL 1200, and INM dives have too few DCS events to produce meaningful results. The saturation dives produce an ODF with ambiguous shape (Figure 5). All bimodal plots have a first peak at 0 hours and a second peak at 2 hours after the final decompression. All ambiguously shaped plots have a peak at 0 hours after the final decompression, however the  $T_1$  and  $T_2$  times documented in these reports are consistent with those that produce bimodal plots.

Dive Trial End Date Range	Dive File	Range Dives Conducted During	Number of Exposures	Number of DCS Occurrences (excluding marginal DCS cases)	ODF Shape Based on Age
1978-1983	EDU1180S	1977-1978	120	10	44 DCS Occurrences Unimodal
	ASATNSM Profiles 14-17	Mar 1977-Feb 1979	23	1	
	DC4W	1978-1983	244	8	
	ASATEDU Profiles 1-5	1979	10	4	
	ASATEDU Profiles 6-9	1979	10	3	
	ASATEDU Profiles 10-12	1979	10	1	
	EDU184	Jul 1980-Aug 1980	239	11	
	ASATEDU Profiles 13-14	1981	10	1	
	ASATEDU Profiles 15-17	1981	11	1	
	ASATNSM Profiles 18-24	May 1979-Feb 1981	12	3	
	ASATEDU Profile 18	1982	10	0	
	ASATEDU Profiles 19-21	1983	10	1	
	ASATEDU Profiles 22-23	1983	10	0	
1984	ASATNSM Profiles 25-28	Sept 1982-Jan 1984	16	1	57 DCS Occurrences Bimodal
	ASATNSM Profiles 1-13	Nov 1983-May 1984	33	4	
	DC4WR	Feb 1984	12	3	
	EDU885A	Aug 1984-Dec 1984	483	30	
	EDU885AR	Aug 1984-Dec 1984	182	11	
	EDU885M	Nov 1984	81	4	
	EDU885S	Dec 1984	94	4	
	ASATEDU Profiles 24-26	1984	10	0	
1985-1987	NMR8697	April 1983-Dec 1985	477	11	43 DCS Occurrences
	ASATNSM Profiles 29-41	Sept 1984-Sept 1986	31	9	Bimodal

	ASATARE	1984-1986	165	20	
	ASATEDU Profiles 27-28	1986	5	1	
	ASATNSM Profiles 42-45	Oct 1986- Jun 1987	17	0	
	ASATEDU Profile 29	April 1987	9	0	
	SUBX87	13-24 July 1987	58	2	
1988-1992	ASATNMR	Jun-Aug 1986, July 1988	50	1	46 DCS Occurrences  Bimodal
	ASATEDU Profiles 30-31	1988	7	0	
	ASATEDU Profile 32	1988	8	1	
	NMRNSW	May 1988- Jan 1989	91	5	
	NSM6HR	1989, 1991	57	3	
	PAMLA 1	Feb 1991- Jun 1991, Jul 1991- Jan 1992	236	13	
	PASA	Mar 1991- Jun 1991	72	5	
	PARA	Jun 1991- Jan 1992	135	7	
	PAMLAOS	Jun 1991- Jan 1992	140	5	
	PAMLAOD	Jun 1991- Jan 1992	134	6	

Table 6. Data partitioned by dive trial chronology [2, 3]. Each dive data file was ordered (and split if necessary) based on dive trial end date. Though the DC4W data file spanned 1978-1986, all eight DCS events occurred during 1978-1983, so this data file has been included in that chronology range. The ASATNMR data file is composed of dive trials during June-August 1986, and then another during July 1988. The 1 DCS occurrence corresponding to these 50 dives occurred during the July 1988 dive trial, so this data file was included in the 1988-1992 range. The ODFs for 1984, 1985-1987, and 1988-1992 are bimodal, with the first peak at 0 hours and the second peak at 2 hours following decompression. The ODF for dive trials completed by 1978-1983 is unimodal, with a peak at 0 hours after the final decompression (Figure 7).

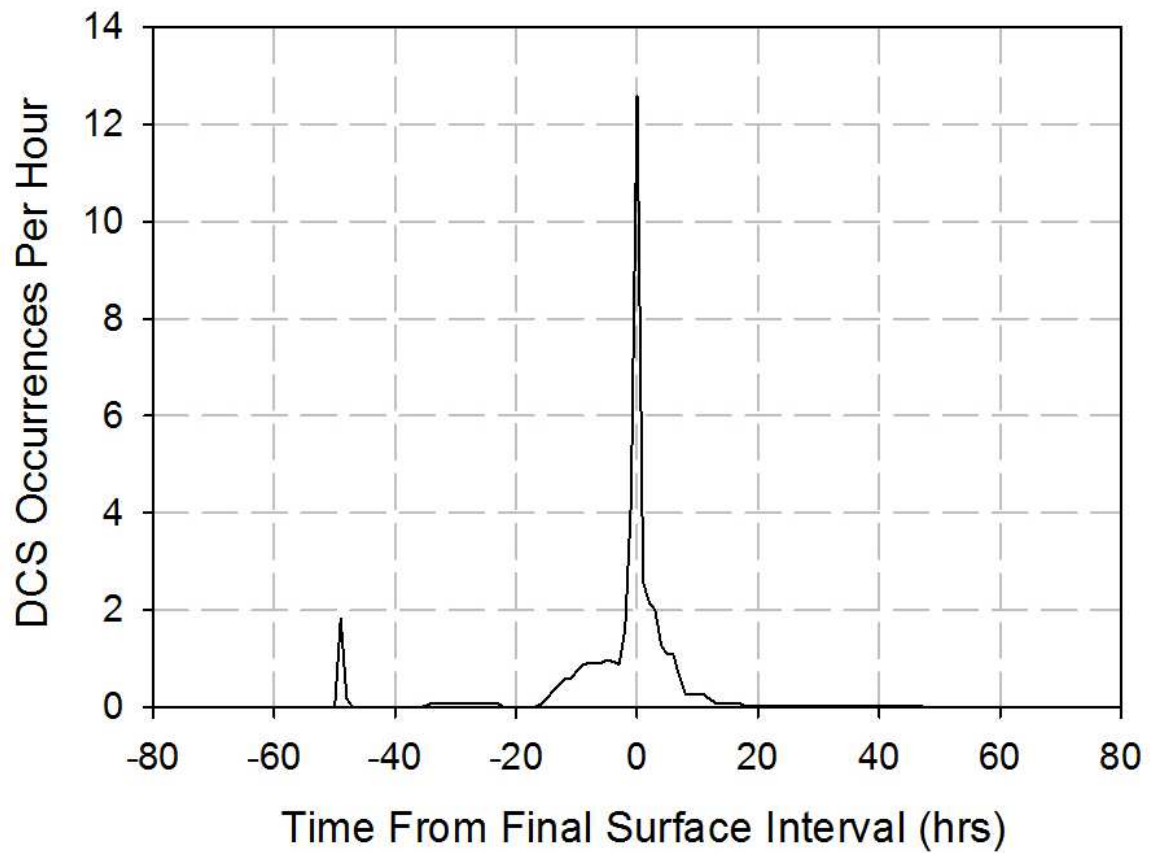


Figure 7. Occurrence density function for dive trials completed during 1978-1983 in the BIG292 data set. See Table 6 for details about dive data files included in this time range. A total of 719 dives were conducted during this time, resulting in 44 DCS occurrences. Neglecting the two cases of DCS that occurred nearly 50 hours before the time of final surfacing, the ODF is unimodal, with a peak corresponding to the time of final surfacing.